TRACKING OCEAN WAVE SPECTRA FROM SAR IMAGES

A. D. Goldfinger
R. C. Beal
F. M. Monaldo
D. G. Tilley
The Johns Hopkins University/Applied Physics Laboratory
Johns Hopkins Road, Laurel, Maryland 20707, USA
Commission II/5

ABSTRACT

For several years we have been working on an end-to-end algorithm for recovery of ocean wave spectral peaks from SAR images. We report on the progress that has been made, and show that current approaches are allowing precision of 1 percent in wave number, and 0.6 deg in direction.

1. INTRODUCTION

A SAR image spectrum is a complex product of the actual ocean wave spectrum, the physics of the scattering process, the SAR instrument, the processing algorithms, and many other effects and parameters. From one or more of these spectra, we seek to either recover the actual ocean wave energy spectrum or to estimate other derived parameters of interest, such as the locations of storm sources.

An overall model is shown in Fig. 1. The left side shows the effects that occur in the production of a SAR spectrum. The right side shows the steps we are undertaking in recovery of information from such a spectrum.

Starting from the actual ocean surface, the physics of the microwave scattering process determines a distribution of scattering cross-section on the sea surface, the so-called "σ_0 map". The physics of this process was the subject of a workshop held at APL in October 1982. We will not discuss this further here but instead refer the interested reader to Beal (1982).

The σ_0 map is viewed by the SAR instrument and three types of corruption occur:

1. Dynamic effects: due to motion of the sea surface, scattered energy is defocused and/or displaced in the SAR image. Both effects serve to decrease azimuth (along-track) resolution, creating a roll-off in the system transfer function for energy with high azimuth wave number. This is described by Monaldo (1983) and Beal, et al. (1983).

2. SAR instrument: the impulse response of the SAR instrument determines a modulation transfer function (MTF), which may vary with time, and certainly is a function of the SAR processor employed.

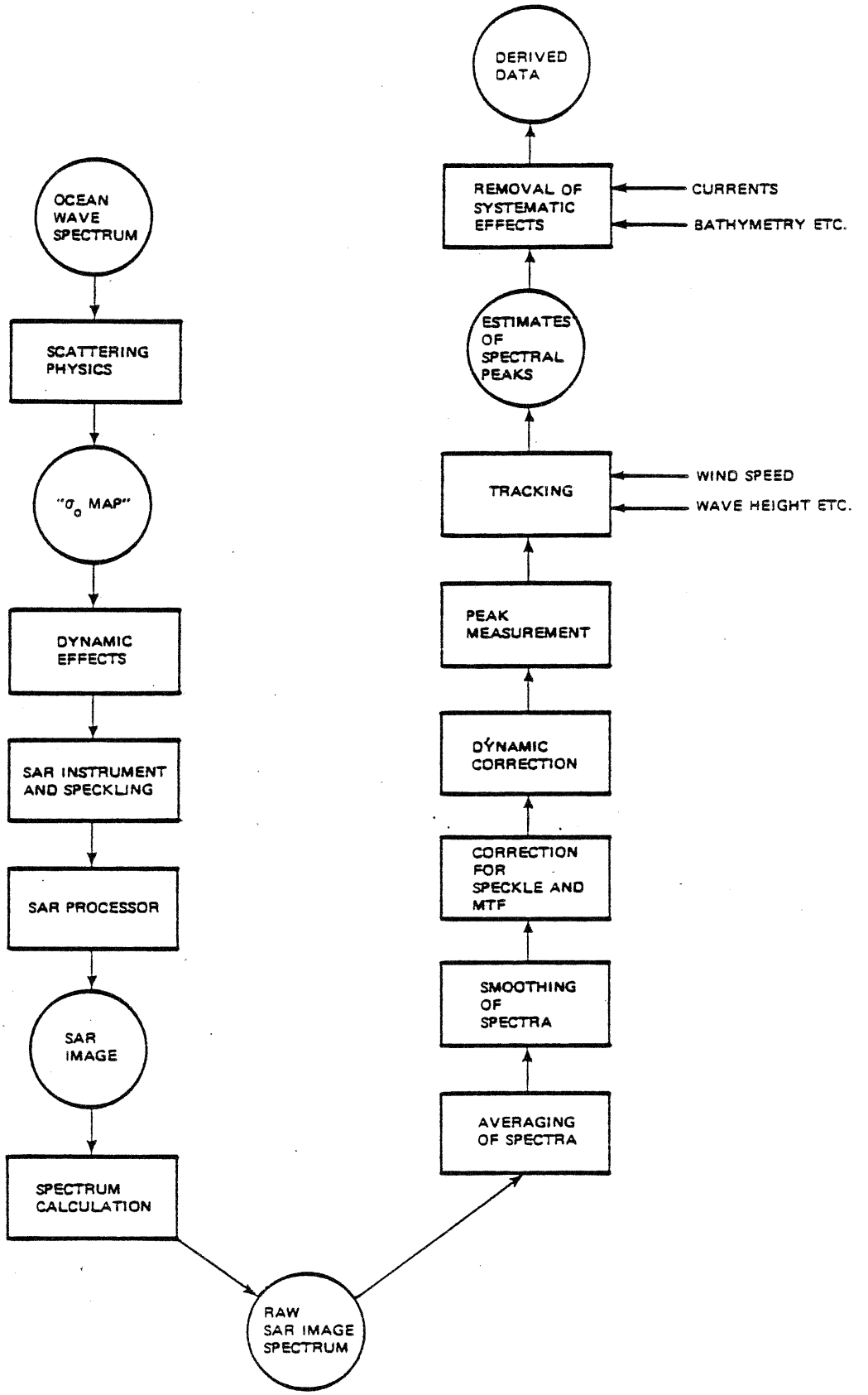

Fig. 1 End-to-end model.

3. Speckle: the coherence of the scattering process results in constructive or destructive interference of the energy returned from each resolution cell. This causes the image to appear speckled. Viewed as an independent process, the effect on image spectra is discussed by Goldfinger (1982). Below, we show what happens when speckling and MTF are considered together.

The final two steps in the production of a SAR spectrum are the computations involved in SAR processing and calculation of the image spectrum. That SAR processor effects are important is demonstrated by Goldfinger (1980).

Armed with the "raw" image spectrum, we go through the series of steps shown on the right side to produce the final estimate of the ocean wave energy spectrum or derived parameters. Since the raw spectra are noisy, it is desirable to average sequential spectra and smooth individual spectra. Following this, the system MTF, which has been estimated by calibration procedures outlined by Beal, et al. (1981), is used to correct for the MTF-speckle effects by an algorithm we describe below. Next, a correction for the dynamic azimuth roll-off is applied, as discussed by Monaldo (1983); and further averaging and smoothing are performed, if needed.

Finally, the spectral peaks are located, measured, and tracked along the pass. The tracking filter to be used can incorporate independent parameters such as wave height or wind velocity in determination of the appropriate filter gains. More will be said of this below.

If derived data, such as storm source position, are desired, it may be necessary to further correct the spectral peak positions for systematic effects such as bathymetry or currents before performing whatever computations are necessary, such as backward and forward extrapolation of wave vectors.

In presenting the above model, we have made the cavalier assumption that the various effects can be separated. For example, we have assumed that the dynamic motion effects can be separated from the SAR instrument and speckling effects. Such assumptions should be regarded as provisional rather than dogmatic. We expect to test each such assumption in turn, and to combine effects when we find they cannot be separated.

For example, in our early work, we assumed that the effects of MTF and speckle could be treated independently. However, a theoretical analysis has shown that this is not true, and hence the two effects are now combined in the model.

2. PROGRESS ON THE PROBLEM

For several years, we have been attempting to understand the above end-to-end process. Our understanding is still incomplete, but partial progress has already been reported in the references. Below, we report on the current status of several items.

2.1 Scattering Physics

Although the "transfer function" due to this process is the subject of current controversy (Beal, 1982), we have found it useful to assume that the relationship between ocean surface slope and radar cross-section is linear. We do so for two reasons:

a. If the transformation between slope and cross-section were strongly nonlinear, then the appearance of higher-order harmonics and intermodulation products of the fundamental ocean frequencies could be expected. Such artifacts have not been observed in SAR image spectra gathered in regions of open water.

b. The primary nonlinear aspect of SAR ocean imagery does not appear to reside in the slope to radar cross-section transformation but rather in the distortion of the SAR image introduced by the presence of ocean surface movement. This nonlinearity, we have shown, can be modeled as a simple resolution loss in a linear system.

Thus, at present, a linear model is still proving useful for the ocean surface slope-radar cross-section relationship.

2.2 Dynamic Effects

It is now well established that wave motion at high sea states causes an azimuth wave number fall-off that tends to rotate the apparent direction of the spectral peaks toward the range (cross-track) direction (Monaldo, 1983). Below, we report the progress we have made in correcting for this effect.

2.3 SAR Instrument and Speckle

The effect of coherent speckle on image spectra in a system with unity transfer function has been treated (Goldfinger, 1982). If $S_0(\underset{\sim}{k})$ is the spectrum of the σ_0 map, the mean SAR image spectrum will be:

$$S'(\underset{\sim}{k}) = S_0(\underset{\sim}{k}) + \frac{1}{N}\int d\underset{\sim}{k}\; S_0(\underset{\sim}{k}) \qquad (1)$$

where N is the number of looks. That is, the mean image spectrum has a bias added that is proportional to the integrated spectral power. The situation becomes more complex when the system modulation transfer function (MTF) is added. The speckle and MTF effects cannot be separated. We have shown that for Gaussian systems:

$$S'(\underset{\sim}{k}) = M(\underset{\sim}{k}) \left[S_0(\underset{\sim}{k}) + \frac{C}{N}\int d\underset{\sim}{k}\; M(\underset{\sim}{k})\; S_0(\underset{\sim}{k})\right] \qquad (2)$$

where M is the MTF and C is a constant. Thus, the spectrum is now weighted by the MTF, as is the power integral taken in the bias term. For non-Gaussian systems, the result is more complex; but analysis of the SEASAT MTF has shown that it is well approximated by a Gaussian, so eq. (2) can be used. Analysis of the statistics of the individual spectra shows that the

assumptions used in deriving eqs. (1) and (2) are valid (Monaldo, 1983).

2.4 SAR Processing Effects

In Goldfinger (1982) and (1980) we have investigated the effects of processor signature in determining system MTF, and shown how to calibrate this aspect of the end-to-end system (Tilley, 1983). We have shown that the total SAR system must be separately calibrated for each SAR processor that is used. This area is now well enough understood that no further work appears necessary.

2.5 Smoothing and Averaging of Spectra

In the averaging of spectra, we encounter a trade-off between averaging more spectra to increase statistical reliability and averaging fewer spectra to examine changes in the ocean spectrum that occur on small spatial scales. Based upon our observation and analysis of data from pass 1339, which covered a 900 x 100 km region off the eastern coast of the United States on September 28, 1978, it was found that spectral variations on the scale of 30 to 40 km tended to be random rather than systematic. Evidence based upon measurement of the correlation distance of the spectrum tended to confirm that these small-scale variations were more characteristic of the instrument and scattering processes than of actual variations of the sea surface. Accordingly, we chose to smooth spectra with a Gaussian kernal extending over about 40 km (i.e., for spectra spaced 6.25 km apart, 15 spectra were averaged along-track with a Gaussian weighting kernal of half width 40 km). This smoothing appeared to be fairly optimal for pass 1339, in that it revealed the local variability caused by the Gulf Stream as well as shallow water bottom features. Whether this will be generally true for other passes remains to be seen. It is important to note that along-track averaging of spectra is not equivalent to along-track smoothing of measured peak positions. The former allows the Gulf Stream to be seen in pass 1339, the latter does not.

In addition to along-track averaging, we have usually applied k-space smoothing to individual spectra. A typical Gaussian smoothing distance was seven wave number intervals. Again a trade-off between resolution and statistical reliability occurs.

2.6 Correction for Speckle and MTF

Based upon eq. (2), we have determined the following algorithm for recovering spectra from a SAR image:

a. Estimate MTF by taking the spectrum of a SAR image of a uniform scene (e.g., a field).

b. Correct the specimen SAR spectra by dividing by MTF and then subtracting a bias.

The efficacy of this algorithm in regions of low to moderate sea state has been reported by Beal and Tilley (1980). The spectral peak positions so obtained have been shown to be highly consistent with known storm sources (Monaldo, 1983). The algorithm is thus well established, except that in cases of high sea state it must be combined with the procedure for azimuth fall-off correction. In general, the correction can be applied only out to azimuth wave numbers well above the noise. The azimuth fall-off problem apparently can be eliminated only by orbiting very low altitude (~ 250 km) SAR systems.

2.7 Dynamic Correction

We have attempted to correct the azimuth fall-off by using a linear semi-empirical model. A Gaussian function in azimuth wave number is fit to a region of the spectrum assumed not to contain any actual spectral power (i.e., the region of very high wave range number). The entire spectrum is then divided by this correction factor.

when this is done, the position of the observed spectral peaks are seen to increase their consistency with known storm sources. Thus, empirical evidence exists which confirms the value of this approach. However, at this time, the procedure and its limitations are still not adequately understood theoretically, a situation we hope to improve in the future.

2.8 Peak Measurement

So far, three algorithms shave been used to determine peak position:

1. Manual: the spectrum is displayed to an operator who uses cross hairs and a joystick to subjectively locate the peak.

2. Automatic/Peak: the peak value of the spectrum is selected automatically.

3. Automated/Center of Gravity: the center of gravity of all pixels exceeding some fraction of the peak is calculated.

Ideally, when presenting spectra to an operator for manual measurement, they should be arranged in random sequence. In our initial study, however, this was not done, and the spectra were presented sequentially. As a result, some "subjective tracking" was performed in obtaining the manual measurements.

At the moment, method 3 appears to be easily feasible, and is at least as accurate as method 1. It does, however, tend to suffer from a bias due to the asymmetric shape of the spectral peak. Method 2 is most noisy.

2.9 Tracking

Most satellite SAR data sets consist of a series of images taken at roughly the same time along an extended swath of ocean coverage. If the scale of ocean variability is large compared to the separation of adjacent images, spectral features can be tracked from one frame to the next with improved accuracy of location.

To date, we have applied both simple smoothing and more complex Kalman filters to the data. We have considered two types of Kalman filter, which we describe as "naive" and "smart". A naive filter treats wave number magnitude and direction as Gauss-Markoff processes with no consideration of their physical origin. Analysis has shown them to be uncorrelated, so we model them as independent. A typical model of wave number magnitude is a random walk in slope, given by the state transition model

$$k_i = k_{i-1} + \dot{k}_{i-1}\,\Delta t \tag{3}$$

$$\dot{k}_i = \dot{k}_{i-1} + w_{i-1} \tag{4}$$

in which w is the driving noise and Δt is the (perhaps variable) along-track spacing between spectra. For proper choices of state and measurement noise parameters, this model is quite successful producing low measurement residuals with a white spectrum. When the model is run "freely", i.e., as a simulation, it produces a random process that looks qualitatively like the wave number excursions we have seen with SEASAT data.

Smart filters take into account the physical origin of the wave number and direction processes. For example, if all waves originate from a point source, such as a localized storm, the following relations will hold,

$$k = \frac{gT^2}{4[r_0^2 - (t-t_o)^2]} \tag{5}$$

$$\theta = \tan^{-1}\left(\frac{t-t_0}{r_o}\right) \tag{6}$$

where g is the acceleration due to gravity, T the time elapsed since the storm, t the along-track position of the spectrum, and r_0, t_0 the range and along-track position of the storm. These relations can be regarded as the nonlinear measurement equation of a three-dimensional state vector: $(r_0, t_0 T)$. Using a simple linear model for propagation of the state, such a random walk in all three parameters, we can construct a nonlinear extended Kalman filter to track storm locations directly from the data as we move along the pass. This model has also proven quite successful, and produces white residuals as small as those produced by the naive filter.

Our work on filtering and tracking continues, but we have been able to reach the following provisional conclusions:

a. On a scale of 10 to 20 km, the variability observed in ocean spectra is due to instrumental or noise effects rather than systematic variation of the ocean waves. Therefore, tracking filters that smooth over such distances will not destroy useful information.

b. The rms errors in spectral peak measurement are dependent upon mean wind speed. A simple linear model ($\sigma^2 = A+BU$, where σ^2 is the error in spectral peak measurement and U is wind speed) has been fit to the data. Therefore, a filter whose gains are dependent on wind speed or other environmental parameters may be of value.

c. Averaging of individual spectra in the along-track direction before estimating spectral peak positions allows small scale phenomena such as the Gulf Stream to be seen. However, neither simple smoothing nor more complex Kalman filtering allow these phenomena to be seen if the along-track averaging is not done. At this moment, we do not have an adequate understanding of this result.

d. Both the naive and smart Kalman filter approaches are valuable, but we do not yet have a basis for preferring one over the other.

3. RESULTS SO FAR

Figures 2 and 3 show the results of a typical application of our end-to-end estimation procedure to the primary spectral peak of pass 1339.

A preliminary analysis of the residuals along the pass shows that spectral peaks can be measured with a wave number precision of .0003 to .0004 rads/m (i.e., ~ 1 percent of mean wave number) and an angular precision of 0.6 deg. We emphasize that this is the result of detailed analysis of a particular wave system over a single pass, and hence, should not yet be generalized to other passes or circumstances.

4. REFERENCES

Beal, R. C. and D. G. Tilley, 1980: Optimal spatial filtering and transfer function for SAR ocean wave spectra. Proceedings of Workshop on SAR Image Quality, ESA Report SP-172, Frascate, Italy.

Beal, R. C., A. D. Goldfinger, D. G. Tilley and W. J. Geckle, 1981: Calibration strategies for spaceborne synthetic aperture radar. JHU/APL Report CP-084.

Beal, R. C., 1982: SEASAT SAR workshop on ocean wave spectra. JHU/APL Internal Report SIR-83U-019.

Beal, R. C., D. G. Tilley and F. M. Monaldo, 1983: Large and small-scale spatial evolution of digitally processed ocean wave spectra from SEASAT synthetic aperture radar. J. Geophys. Res., 88, (C3), 1761-1778.

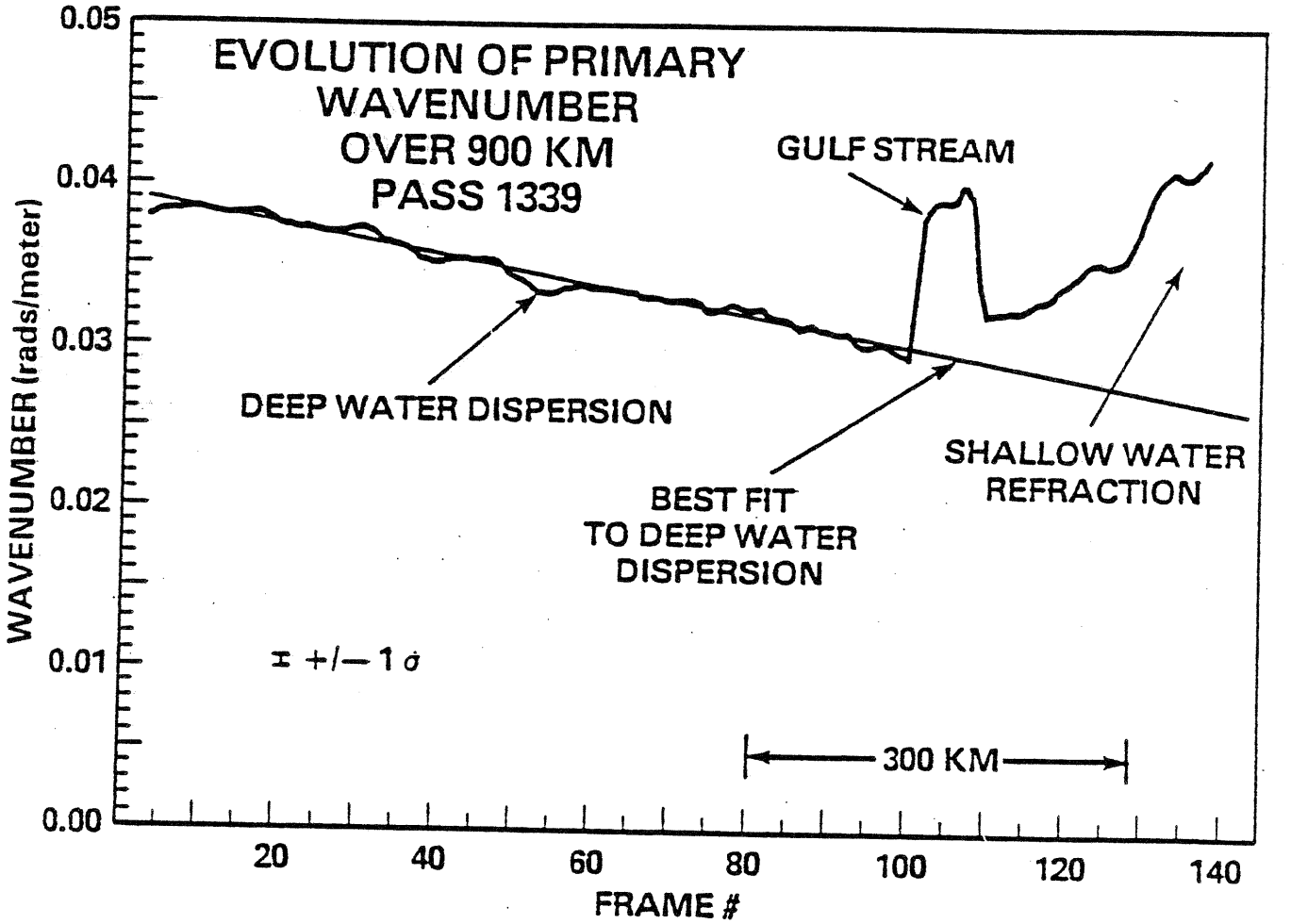

Fig. 2 Wavenumber variation.

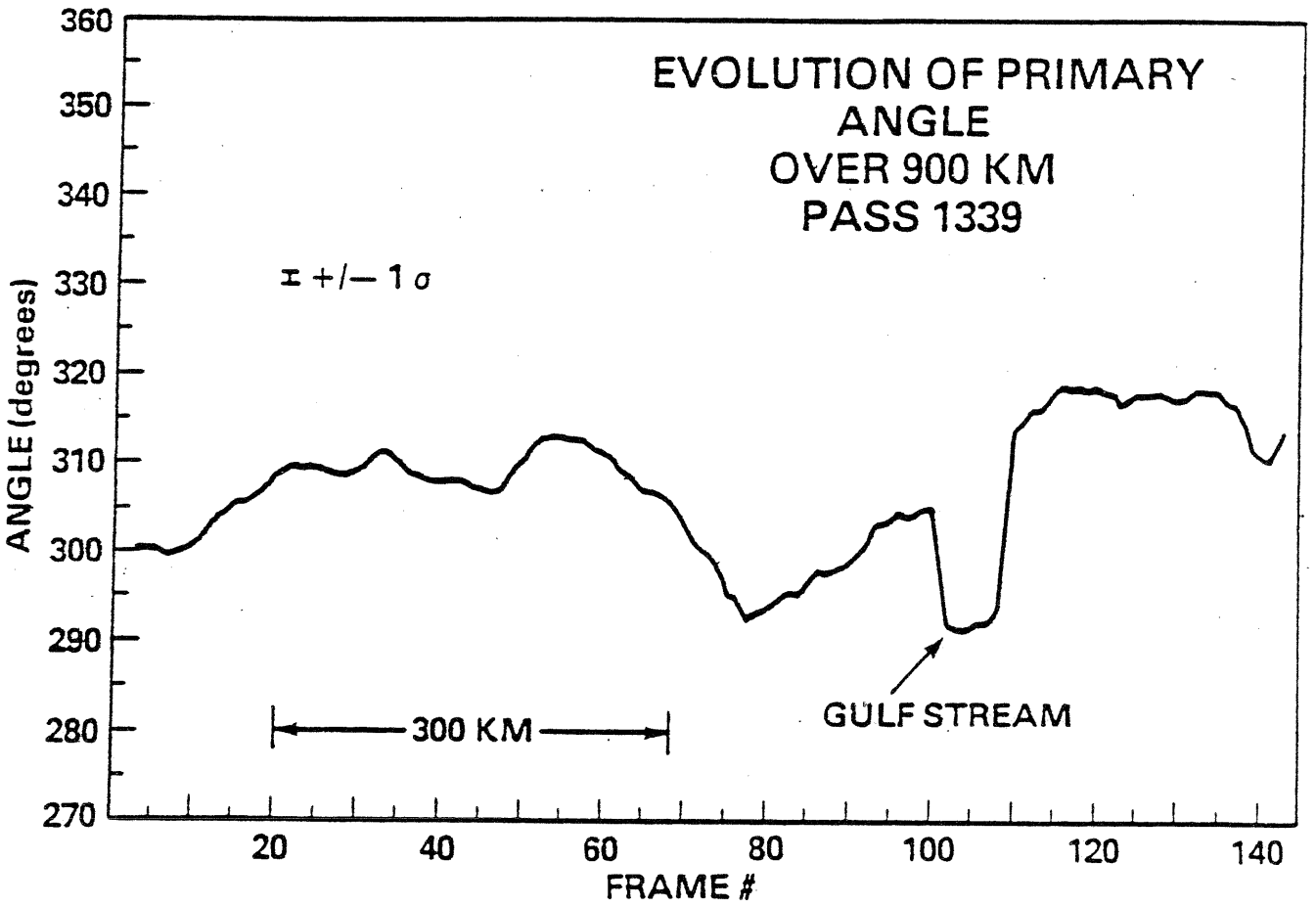

Fig. 3 Angle variation.

Goldfinger, A. D., 1980: SEASAT SAR processor signatures: Point targets. JHU/APL Report CP-078.

Goldfinger, A. D., 1982: Estimation of spectra from speckled images. IEEE Trans. on Aerospace and Electronic Systems, Vol. AES-18, 675-681.

Monaldo, F. M., 1983: Tracking ocean surface waves using spaceborne SAR image spectra corrected for ocean surface movement. Proc. 1983 IGARS Symposium.

Tilley, D. G., 1983: Fourier analysis of SAR speckle for polynomial synthesis of spectral corrections applied to SEASAT oceanic data. Proc. 1983 IGARS Symposium.